J Fluoresc (2013) 23:1065–1076
DOI 10.1007/s10895-013-1236-4

ORIGINAL PAPER

Elucidation of Monomerization Effect of PVP on Chlorin e6 Aggregates by Spectroscopic, Chemometric, Thermodynamic and Molecular Simulation Studies

Shubhajit Paul · Susithra Selvam · Paul Wan Sia Heng · Lai Wah Chan

Received: 27 March 2013 / Accepted: 9 May 2013 / Published online: 17 May 2013

Abstract Molecular aggregation in aqueous media is one of the factors which largely affects the efficacy of photosensitizers in photodynamic therapy. Chlorin e6 (Ce6) in aggregated form is known to exhibit markedly reduced therapeutic effects. In the present study, aggregate to monomer conversion of Ce6 was investigated as a function of pH and polyvinylpyrrolidone (PVP) concentration by simple absorption and fluorescence spectroscopic techniques. Aggregation of Ce6 was observed in the pH range of 2 to 6 as indicated by changes in UV–vis absorption spectra, fluorescence emission spectra and relative quantum yield. Novel chemometric approach was considered for determining the relative monomerization efficiency of different grades of PVP. The chemometric analysis and binding constant study both strongly revealed that the Ce6-PVP complex was more efficiently formed with PVP of the lowest molecular weight (K17). Thermodynamic parameters, such as the heat of entropy and enthalpy, showed that complex formation was largely attributed to hydrophobic interaction between Ce6 and PVP. This was found to be consistent with the results obtained from molecular simulation study.

Keywords Chlorin e6 · Aggregation · Fluorescence spectroscopy · Complexation · Polyvinylpyrrolidone K17 · K25 · K30 · Dynamic simulation

S. Paul · P. W. S. Heng · L. W. Chan (✉)
Department of Pharmacy, Faculty of Science,
National University of Singapore, 18 Science Drive 4,
Singapore 117543, Singapore
e-mail: phaclw@nus.edu.sg

S. Selvam
Department of Chemistry, Vel Tech Dr. RR and Dr. SR
Technical University, Tamil Nadu, India

Introduction

Photodynamic therapy (PDT) for the treatment of cancer has been a growing field of interest over the last 25 years [1]. This mode of therapy is based on selective localization of photosensitizers in tumor cells and subsequent destruction of the tumor cells upon excitation of the photosensitizers [2]. The ideal characteristics of a photosensitizer for use in PDT include high penetration into the target tissue, tumor selectivity and high quantum efficiency for singlet oxygen generation. Due to better penetration of red light through the tissues, strong absorption in the visible spectrum is a desirable property of the photosensitizers [3]. Target delivery of photosensitizers using a suitable carrier is a promising approach in the treatment of cancer [4]. Porphyrins are the most commonly used photosensitizers in PDT. These are highly conjugated heterocyclic aromatic compounds composed of four modified pyrrole subunits. As a consequence, they have intense absorption bands in the visible region and strong fluorescence emission characteristics [5]. Over the years, porphyrins have been delivered in various nanoparticulate forms for the treatment of cancers [6]. Chlorins, a class of porphyrins, exhibit a large extinction coefficient in the afore-mentioned spectral region. In addition, it has been shown that molecules with chlorin type structure are able to sensitize generation of singlet oxygen with a high quantum yield [7]. Chlorin e6 (Ce6), shown in Fig. 1 is a promising photosensitizer characterized by high sensitizing efficacy and rapid elimination from the body [8]. At one end of this molecule, several alkyl groups are present, which renders the molecule hydrophobic in nature. Three peripherally attached carboxylic groups are present at the other end, which exists in different ionic forms depending on the pH. Such amphiphilic property leads to one potential disadvantage of Ce6, which is molecular

aggregate formation and this reduces the sensitizing efficiency during PDT. Preliminary studies have suggested that Ce6 aggregates predominate under acidic pH conditions whereas the monomeric form exists under alkaline pH conditions [9]. The aggregates tend to lower the sensitizing efficiency and therefore affect the therapeutic efficacy of the photosensitizer. Photophysical properties of Ce6-PVP formulations have been described by Isakau et al. in terms of photophysical and physicochemical parameters, such as solubility, partition coefficient, triplet-triplet absorption and time correlated fluorescence spectroscopy [10]. The study revealed that Ce6 interacted with PVP to form molecular complexes and this prevented Ce6 aggregation in aqueous media, leading to an enhancement of Ce6 fluorescence quantum yield. The disaggregated Ce6 associated with PVP was found to have therapeutic activity greater than that of the aggregated Ce6 molecules. Photolon® (also known as Fotolon®), a formulation containing a complex of Ce6 and PVP at the ratio of 1:1 (w/w) has been established to be effective in photodynamic diagnosis and treatment of different cancerous and non-oncological diseases [11–14]. The disadvantage of the aggregation of Ce6 can be overcome by synthesizing water-soluble derivatives of Ce6 [15, 16]. However, this method is less preferred as the synthesis involves complicated steps and the need for new regulatory approvals.

A better understanding of the phenomenon of monomerization of Ce6 is necessary because of its pharmaceutical relevance in PDT. Some important findings on the photophysical changes of Ce6 in the presence of PVP and the Ce6-PVP binding mechanism had been reported by Isakau et al. [10]. In the present study, further investigation to elucidate the aggregation and disaggregation phenomena of Ce6 by simple spectroscopic techniques was carried out. The binding mode was directly determined using thermodynamics and binding mechanism was demonstrated by molecular dynamics simulation. In addition, the disaggregation efficiency of PVP of various molecular weight grades was further illustrated using chemometrics such as parallel factor (PARAFAC) algorithm. The findings will be useful in the formulation of Ce6 with suitable grades of PVP to achieve optimal activity in PDT.

Materials and Methods

Materials

Chlorin e6 (97.8 % pure) was purchased from SPE Chemicals (Shanghai, China). Three grades of polyvinylpyrrolidone (PVP: K17, K25 and K30, ISP Pharmaceuticals, Wayne, NJ, USA) were used. Their average molecular weights are stated in Table 1. All the other reagents used for the preparation of buffered solutions were of analytical grade.

Preparation of Test Solutions for the Different Studies

A fixed concentration of Ce6 (50 μM) was selected for pH- and PVP- induced disaggregation study. A series of solutions ranging from pH 1.2 to 10 was prepared using potassium dihydrogen phosphate, phosphoric acid and sodium hydroxide according to the USP method. Chlorin e6 was dissolved in 0.1 % NaOH solution to prepare a stock from which 30 μL was withdrawn and added to each of the different pH solutions (pH 1.2 to 10) to produce a final Ce6 concentration of 50 μM in 5 mL. For the PVP-induced disaggregation study, different amounts of PVP were added to 50 μM Ce6 solutions at specified pH conditions to give Ce6 to PVP ratios of 1:10 to 1:1000. The respective solutions were placed in a bath sonicator for 5 min and measurements were conducted immediately thereafter.

Measurement of Absorption and Fluorescence

The absorption and fluorescence spectra were recorded using uv-visible spectrophotometer (Shimadzu, UVPC 2010, Kyoto, Japan) and spectrofluorimeter (Fluoromax-P, Jovin Yvon, Edison, NJ, USA) respectively. The excitation and emission slits were set at a bandwidth of 2.0 nm.

Collection of 3D Fluorescence Spectra

3D fluorescence spectra of Ce6 in the presence of different concentrations of each PVP grade were collected from 600 nm to 750 nm, in 2 nm increments, at increasing excitation wavelengths from 390 nm to 690 nm, in 5 nm increments, with an excitation and emission slit width of 2 nm. Multivariate curve resolution of the obtained spectra was accomplished in Matlab software (mathworks Inc., Nattick, NJ, USA). PARAFAC algorithm was thereafter employed to determine the number of species and there corresponding proportions of Ce6 at varying concentrations of each of the PVP grades.

Fluorescence Quantum Yield

Fluorescence quantum yield (Φ), which represents the activity of a fluorophore, is defined by the ratio of number of photons emitted to the number of photons absorbed. The relative quantum yields of Ce6 at different pH conditions were calculated using the following equation [17]:

$$\frac{\emptyset_1}{\emptyset_2} = \frac{\left(1-10^{A2}\right)\varphi_1^2\alpha_1}{\left(1-10^{A1}\right)\varphi_2^2\alpha_2} \quad (1)$$

where, A is the absorbance in the solvent, φ is the refractive index of the solvent and α is the area under the fluorescence

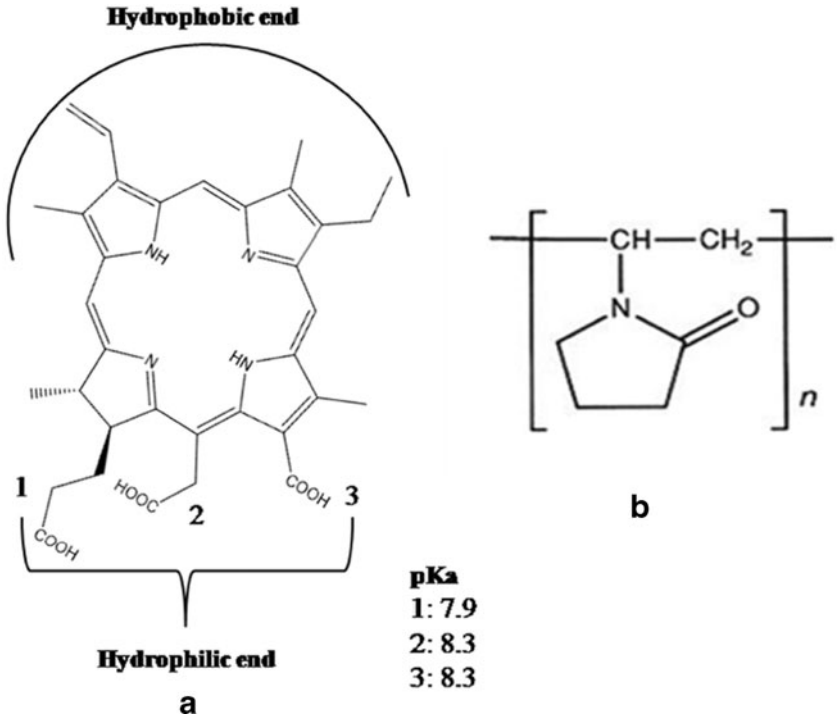

Fig. 1 Chemical structures of **a** Chlorin e6 and **b** Polyvinylpyrolidone

emission curve, with 1 and 2 representing the test and standard samples respectively. In the present study, the quantum yield of Ce6 at pH 10 was set at 1.0 and the relative quantum yields at other pH conditions were determined. It was assumed that Ce6 existed primarily as monomers at pH 10 and exhibited the highest quantum yield.

Ce6-PVP Binding Study

The binding of Ce6 with PVP was evaluated at physiological pH 7.4 at low Ce6 concentrations (~ 10 μM), where Ce6 molecules preferentially existed in monomeric forms [10]. Binding constants and the number of binding sites for different PVP grades were determined using a simple model based on drug-polymer binding [18]. This model assumes that the ligand molecule has similar affinity for each of the monomer units that form the polymeric macromolecule.

Table 1 Binding parameters of Ce6 with PVP of different molecular weights

PVP Grade	M_w[a]	K_a ($\times 10^4$ mol^{-1})[b]	p[c]	N_o[d]
K17	10,000	3.66±0.8	61±4	1.62±0.2
K25	24,000	3.51±0.6	53±4	4.23±0.3
K30	41,000	3.34±0.6	37±7	8.07±0.8

[a] average molecular weight of the PVP grade

[b] binding constant

[c] number of monomer units required to constitute one binding site

[d] mean number of binding site per PVP molecule

Depending on the ligand molecular size, molecular weight of polymer and length of monomer unit, each ligand molecule may bind with one or several monomer units [19]. In the present study, Ce6 and PVP were designated as drug and polymer respectively. The fraction of Ce6 bound with PVP (x) was determined from the absorbance values of the test system to which increasing amount of PVP was added, where Ce6 would bind with PVP in increasing extent and fully at the maximum PVP concentration employed. Linear superposition was applied by assuming that the Ce6 absorbance (D) at a given PVP concentration is a linear superposition of the absorbance of fully free (D_1) and fully bound (D_2) Ce6 molecules:

$$D = x.D_2 + (1-x).D_1, 0 < x < 1 \quad (2)$$

Therefore, the concentration of PVP-bound Ce6 (C_B) is given by:

$$C_B = x \times C_T = \frac{D-D_1}{D_2-D_1} \times C_T \quad (3)$$

Free or unbound Ce6 (C_F)=C_T -C_B, where C_T is the total Ce6 concentration, which is a known quantity. Therefore, number of moles of Ce6 bound per mole of PVP monomer unit, r is given by:

$$r = \frac{C_B}{[PVP]} \quad (4)$$

The binding constants and number of binding sites for different PVP grades were calculated using the slope and

intercept of the Klotz double reciprocal plot given by [18]:

$$\frac{1}{r} = \frac{1}{n} + \frac{1}{nK_a C_F} \quad (5)$$

where n (>1) is the number of binding sites per mole of monomer unit and K_a is the binding constant. When the ligand molecule is large and the molecular weight of monomer unit is low, n is much smaller than 1. The term p ($1/n$) represents the number of monomer units required to constitute one binding site. The mean number of binding sites per PVP molecule is given by:

$$N_0 = \frac{W}{W_{momo}} \times n \quad (6)$$

where W and W_{mono} are the molecular weight of the PVP polymer and each monomer unit respectively.

Ce6-PVP Binding Mode Study

Ce6-PVP binding mode study was conducted at three specified temperatures, 15 °C, 24 °C and 37 °C. The binding constant (K_a) value was obtained from spectroscopic measurements at each of the temperature mentioned above using Eqs. (2) to (5). These different K_a values were plotted against the corresponding temperature to calculate the thermodynamic parameters as shown by Van't Hoff's equation [19]:

$$\mathrm{In}K_a = -\frac{\Delta H}{RT} + \frac{\Delta S}{R} \quad (7)$$

where K_a is the binding constant at each of the specified temperature points (for each of the PVP grades) while ΔH and ΔS are the changes in enthalpy and entropy of the system and R is the gas constant. Binding constant values obtained at different temperature points were plotted against 1/T and the thermodynamic parameters were calculated from the slope and intercept of the plot [20]. The free energy change (ΔG) was estimated from the following relationship:

$$\Delta G = -RT\mathrm{ln}K_a = \Delta H - T\Delta S \quad (8)$$

All the spectroscopic measurements were conducted at room temperature (24 °C). For the thermodynamic study, two additional temperature of 15 °C and 37 °C were employed.

Molecular Dynamics Simulation

Molecular dynamics simulation was performed using Hyperchem 8.0 (Hypercube Inc., Gainesville, FL, USA). Repeating monomer unit of PVP was built using Polymer builder toolbox of Materials Studio 5.0 (Accelrys Inc., San Diego, CA, USA) and a model PVP polymer with 20 repeating units was generated. The Ce6 structure was constructed using Chemdraw software (Version 7.0, Perkin Elmer informatics, Cambridge, MA, USA). Ce6 and PVP structures were then optimized by PM3 (modified Austin model) parameterization using Hyperchem software. The individual molecules were subjected to complete energy minimization in periodic boundary of dimensions 20-15-40 Å (x-y-z) containing 483 water molecules. An AMBER force field and Polak-Ribiere conjugate gradient optimizer were used for the molecular dynamics simulation. In the present study, a run time of 0.6 ps was selected with an initial heat time of 0.1 ps to increase the temperature of the system from 100 K to 300 K in 30 K steps. The free energy was calculated after the simulation run and molecular orientation of Ce6-PVP complex was demonstrated.

Results and Discussion

Spectral Features of Ce6 at Different pH

The influence of pH was investigated over a range from pH 1.2 to 10 using 50 μM Ce6, which was reported to be a moderate concentration in previous studies [7, 21]. This concentration was also within the range above which self-absorption or scattering was observed in the absorption and fluorescence spectra, respectively. The absorbance spectra of Ce6 under the specified pH conditions are shown in Fig. 2. Preliminary study suggested that a strong Soret band (at about 400 nm) and less intense Q bands in the visible region (650–700 nm) are characteristic absorption peaks of Ce6. These features are similar to those of porphyrins. The Ce6 molecule has ionizable groups attached to its ring system, thereby existing in different ionic forms depending on the pH of the medium. The ionization of the carboxylic groups of Ce6 has been reported to occur within neutral (6.8) to alkaline pH [22]. Therefore, it was hypothesized that in the acidic pH condition, the non-ionized carboxylic groups formed intermolecular H-bonds and facilitated aggregate formation. Upon ionization in alkaline pH, aggregate formation was impaired, resulting in monomer-rich Ce6. Figure 2 shows the spectral shifts in Soret and Q bands over the pH range of 1.2 to 10. The wavelength of the absorption maxima (λ_{max}) for the Soret and Q bands in water (pH 6.8) was found to be 404 nm and 653 nm respectively (Fig. 2a and c). On increasing the pH from 6.8 to 10, the λ_{max} for both the Soret and Q bands were unaffected but their absorbance significantly increased (Fig. 2a and c). Interestingly, significant spectral changes were observed for both Soret and Q bands when the pH was varied from 6.8 to about 1.2. Soret band exhibited a red shift from 404 nm to 409 nm while the Q band consisted of a sharp peak at 642 nm (peak 1) and another small hump at 673 nm

(peak 2). The intensity also generally decreased on decreasing the pH of the solution (Fig. 2a and b). A less broadened Q band, devoid of any hump at pH 1.2 was observed, which implied reduced aggregation state of Ce6. At very low pH, the imino nitrogens in the pyrrole ring of porphyrin nucleus are protonated, which could result in repulsion of adjacent Ce6 molecule, thereby dispersing the Ce6 aggregates [23].

From the corresponding fluorescence spectrum, the wavelength of maximum emission (λ_{em}) was obtained at 656 nm with an excitation wavelength of 405 nm (Fig. 3). On increasing the pH from 6.8 to 10, λ_{em} remained the same at 656 nm but the fluorescence intensity increased significantly. The fluorescence emission peak maxima exhibited a blue shift from 656 nm to 644 nm when the pH was decreased from 6.8 to 3.0. Further decrease in pH to 1.2 increased the λ_{em} to 651 nm. Nonetheless, fluorescence intensity gradually decreased with decreasing pH in the pH range 2 to 6.

A broad absorption spectrum accompanied by blue shift in Q band in the pH range 2 to 6 indicates aggregation of Ce6 in the acidic pH conditions. From the fluorescence emission spectra, the Ce6 species found in acidic pH (pH 2 to 6) was different from that found in near neutral to alkaline pH. The fluorescence spectra of Ce6 aggregates in acidic pH condition showed a blue shift and reduced fluorescence emission intensity. These observations corroborated earlier findings that Ce6 existed in two different forms, predominantly as aggregates in acidic pH and monomeric form in alkaline pH [24].

Studies conducted by Isakau et al. showed that Ce6-PVP complexes had higher quantum yield than Ce6 aggregates [10]. In this study, the influence of pH on the quantum yield was further investigated to demonstrate the microenvironmental polarity change at different pH conditions. Figure 3 shows that Ce6 particularly in the alkaline pH conditions had higher fluorescence intensity, which was almost double than that in acidic pH conditions of similar Ce6 concentrations. This suggests that the quantum yield of Ce6 was significantly affected by pH. Relative quantum yield measurement was conducted in the present study, as it is a simple approach that does not require any standard dye. The quantum yield of Ce6 in pH 10 was assumed to be the highest possible and therefore assigned a value of unity. The relative quantum yields of the others were subsequently determined using Eq. (1) [25]. Figure 4 shows the relative quantum yield of Ce6 in different pH conditions. The quantum yield increased slightly from pH 2 to 6, followed by a steep increase above pH 6. It has been reported that a reduction in quantum yield could be caused by a nonspontaneous excited state transformation, resulting in a decrease in singlet oxygen generation [26]. Hence, it could be inferred that the aggregated Ce6 molecules drastically reduced the quantum yield values with a subsequent decrease in sensitizing efficacy. The influence of pH on quantum yield of Ce6 was largely mediated through its effect on Ce6 aggregation.

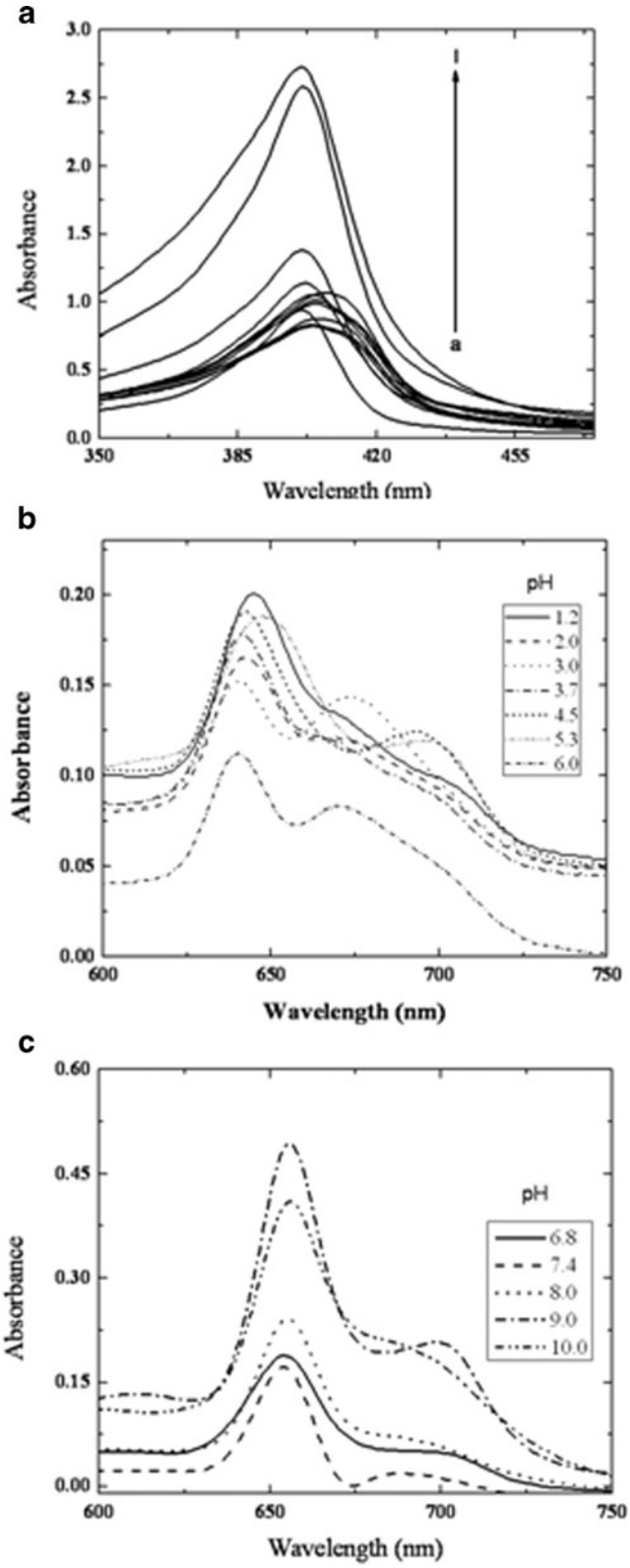

Fig. 2 Absorbance of **a** Soret band (pH, a to *I*=1.2 to 10) and Q band in **b** acidic and **c** neutral to alkaline pH

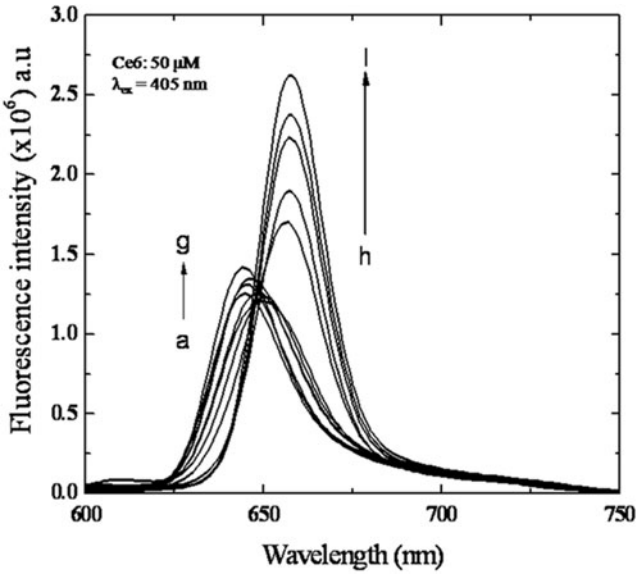

Fig. 3 Effect of pH on fluorescence emission spectra of Ce6 (pH, a to *g*=1.2 to 6.0, h to *l*=6.8 to 10.0)

From the pH study, Ce6 was found to exist preferentially in aggregated form in the pH range of 2 to 6. As the tumor microenvironment is generally acidic in nature, this study demonstrates the importance of formulation to minimize Ce6 aggregation in order to achieve higher photodynamic efficacy [27].

Monomerization of Ce6 Aggregates Using PVP

PVP K25 is widely used in the formulation of drug delivery systems [28]. PVP was reported to induce monomerization of Ce6 aggregates. However, information on the effect of PVP of different molecular weights on the various photophysical properties of monomerized Ce6 species is lacking. In this study, different grades of PVP were used to investigate the effect of PVP molecular weight on monomerization of Ce6 aggregates. It is ideal to conduct disaggregation study of Ce6 using PVP at relevant tumour physiological pH condition, the typical value of which lies around pH 6.6–7.0. However, studies showed that the pH could be lower in certain cases [29]. Moreover, a recent study on breast cancer model revealed the very low pH (≤ 5.0) in lysosomes, where chlorin photosensitizers were reported to accumulate and exert phototoxic activity [30]. Hence, the present study investigated the effect of varying pH on the disaggregation efficacy of PVP. The ionization of carboxylic acid groups in the alkaline pH suggests increasing solubility of Ce6 with decrease in hydrophobic interaction, leading to lower propensity for aggregate formation. At higher pH (near-neutral to alkaline), Ce6 was relatively polar and less aggregated. Thus, it could be anticipated that the disaggregating effect of PVP in the acidic pH region was more challenging due to the presence of higher fraction of aggregated Ce6. From the pH study, the extent of aggregation was mainly observed from pH 2 to 6. Hence, the effect of PVP K25 on the monomerization of Ce6 aggregates in this pH range was thoroughly investigated. Variation in fluorescence emission spectra over pH 2 to 6 followed a notable trend, indicating that the use of any pH condition within 2 to 6 for comparative disaggregation study would be acceptable. Therefore, further studies were carried out using the different grades of PVP at pH 5 to simulate the tumour physiological environment. Figure 5(a) shows the effect of increasing concentration of PVP K25 on the Q band. Q band shows 2 peaks: peak 1 (λ_{max} at 642 nm) and peak 2 (λ_{max} at 673 nm). Interestingly, peak 2 became more prominent with the addition of PVP K25. The absorbance of peak 1 remained relatively constant, whereas the absorbance of peak 2 gradually increased as the PVP to Ce6 ratio changed from 10:1 to 1000:1. The evolution of characteristic peak 2 by the action of PVP indicated its monomerization effect on Ce6. The concomitant increase in peak 2 intensity with increasing PVP K25 concentration was consistent throughout the pH range of 2 to 6 (Fig. 5b). As can be seen, the ratio of peak 2 (A_{673}) to peak 1 (A_{642}) gradually increased up to PVP to Ce6 ratio of 100:1. Figire 5(c) shows the variation of the ratio of peak 2 to peak 1 absorbance for all the PVP grades at pH 5. A linear dependence between A_{673}/A_{642} to PVP:Ce6 ratio was generally observed up to PVP to Ce6 ratio of 100:1. Further addition of PVP resulted in stabilization of peak 2 intensity, indicating slight increase in A_{673}/A_{642} ratio compared to high amount of PVP present in the system. This was consistent for all the grades of PVP, suggesting significant monomerization of Ce6 aggregates was mostly achieved at PVP to Ce6 ratio of 100:1 and finally the binding sites of PVP was completely saturated at a PVP to Ce6 ratio of 1000:1. This is an important observation and it could be regarded as an index of monomerization of Ce6 aggregates.

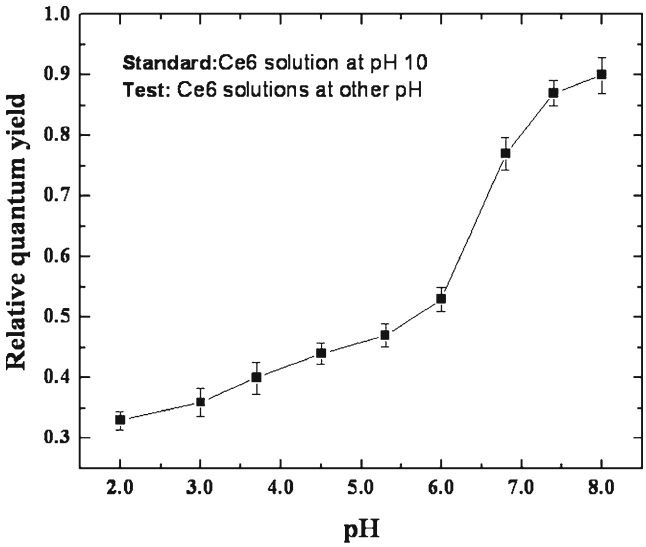

Fig. 4 Effect of pH on relative quantum yield of Ce6

Figure 6 shows the fluorescence emission spectra at various Ce6 to PVP ratios at pH 5 for PVP K25. Two interesting observations were noted here. Firstly, on addition of PVP, fluorescence intensity decreased and the emission spectra exhibited a bathochromic shift. At a moderate PVP to Ce6 ratio (100:1), two emission peaks were observed, with one peak at 645 nm and another at 665 nm when excitation wavelength was set at 405 nm. On further addition of PVP, the peak at 645 nm gradually diminished and at a very high PVP concentration (PVP to Ce6 ratio of 500:1), only an intense peak at 672 nm was observed. No further change in peak position was observed up to PVP to Ce6 ratio of 1000:1 implying all the Ce6 molecules were eventually converted to monomers. Similar spectral changes were also observed with PVP K17 and K30 (figure not shown). Such observation implies that there could be three different Ce6 species present, notably pure Ce6 aggregates (λ_{em}: 645 nm), Ce6 partially bound to PVP or intermediate species (λ_{em}: 665 nm) and pure Ce6 monomers, completely bound to PVP (λ_{em}: 672 nm). It was also observed that PVP was non-fluorescent when excited at 405 nm (figure not shown). Thus, the decrease in fluorescence intensity could be ascribed to higher probability for triplet excited state attainment of Ce6 monomers than singlet ground state. In addition, bathochromic shifts are associated with increase in microenvironment polarity, which may be brought about by conversion of aggregates to monomers. Collectively, the results indicate monomerization of Ce6 aggregates by complex formation between Ce6 and PVP. Ce6 would bind to certain sites of the PVP molecule, thereby overcoming Ce6 aggregation. At very high PVP concentration, all the Ce6 molecules were bound to PVP and no further shift in emission spectra was observed.

In summary, the monomerization effect of PVP on Ce6 has been demonstrated by changes in absorption and fluorescence spectra. On addition of PVP, both Q band and fluorescence emission peak (λ_{em}) exhibited a bathochromic shift, implying a more polar environment for Ce6. The latter was attributed to monomerization of Ce6 aggregates by complex formation between Ce6 and PVP.

Determination of Relative Disaggregation Efficiency from PARAFAC Analysis

The relative disaggregation efficiency of the different PVP grades was determined from the PARAFAC analysis. 3D fluorescence spectroscopy has gained interest in recent years owing to their suitability to accurately quantify and predict the individual components in a set comprising of mixture of components. The process involves exciting a sample over a range of wavelengths and recording the fluorescence emission over another range of wavelengths [31, 32]. Combining the data produces a contoured map, often referred to as a

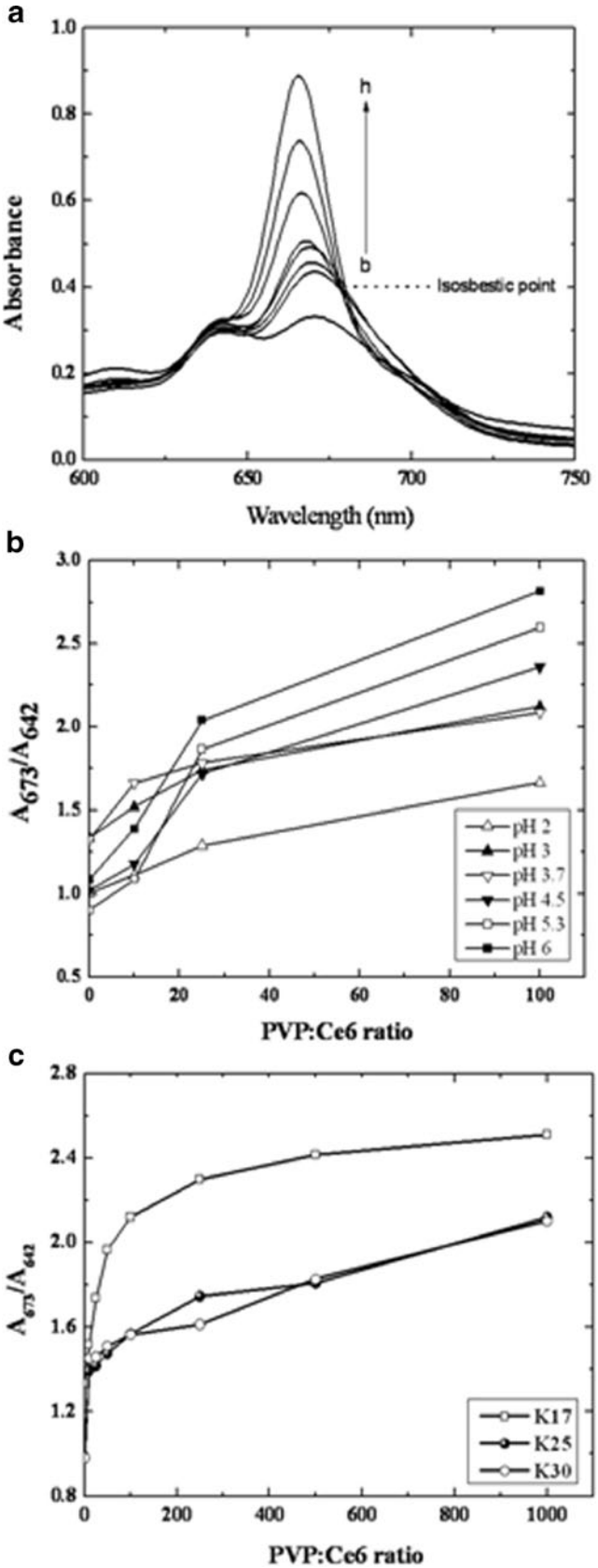

Fig. 5 **a** Q band characteristics on addition of PVP K25 at pH 5 (PVP:Ce6, a to *h*=0 to 1000); effect of **b** pH and **c** PVP molecular weights on the ratio of absorbance between 673 nm and 642 nm

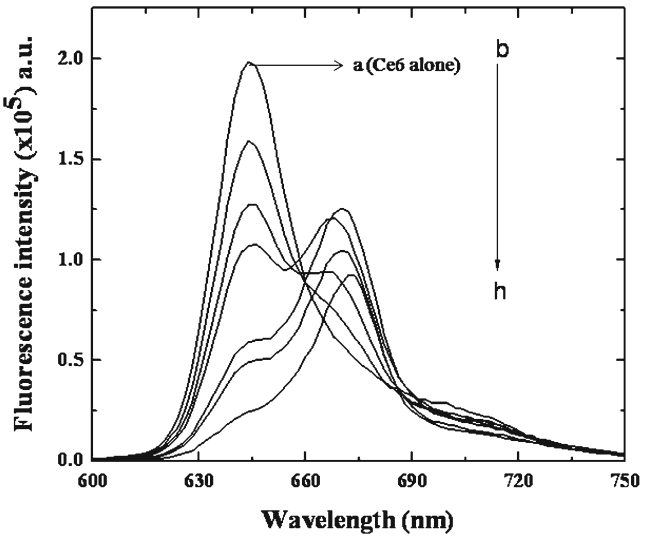

Fig. 6 Effect of PVP K25 on Ce6 emission spectra (PVP:Ce6, *a*=0, *b*=10, *c*=25, *d*=50, *e*=100, *f*=250, *g*=500, *h*=1,000)

"fingerprint", displaying fluorescent peak locations and intensities. The peak locations indicate the type of fluorescent substance (different species) and the intensity represents the concentration. PARAFAC is a powerful chemometric method, which has been successfully used in the analysis of multi-way data to determine both qualitative and quantitative information. PARAFAC is based on the trilinear model, given by [33]:

$$r_{i,j,k} = \sum_{n=1}^{N} x_{i,n} y_{i,n} z_{i,n} + e_{i,j,k} \quad (9)$$

where $r_{i,j,k}$ represents the measured response of the *k*th sample at the *i*th excitation and *j*th emission wavelengths. In this study, each *k*th slice of the trilinear data cube R represents one EEM fluorescence spectrum in a series of samples and has the dimensions of I, J, where I is the number of excitation wavelengths and J is the number of emission wavelengths. The number of factors, *N*, chosen to model the system, is defined by the user.

From prior observation, the addition of PVP resulted in 3 distinct peaks in Ce6 fluorescence spectra. The correlation coefficient (r) of the estimated proportion of different species was found to be higher (0.982) using *N* equal to 3 instead of 2 (0.935) for PVP K25 dataset. Therefore, the PARAFAC analysis for different grades of PVP was conducted using *N* as 3. As can be seen from Fig. 7, the proportion of Ce6 aggregates varied significantly for different grades of PVP with their increasing concentrations. It was found that the K17 grade had the maximum efficiency to convert the aggregates into monomeric form at minimum PVP concentration (PVP:Ce6 ratio=10:1). At the similar concentration, the efficiency gradually decreased in the following order: K17>K25>K30. However, on increasing PVP concentrations, aggregates were gradually converted to monomers and at maximum PVP to Ce6 ratio (1000:1), all the aggregates were mostly converted to PVP-bound monomeric forms. This apparently suggested that at lowest PVP concentration, PVP K17 had the maximum monomerization efficiency amongst the three grades. Similar findings were observed in the binding constant study and the probable reason is discussed in the following section.

Ce6-PVP Binding Constant Study

As mentioned earlier, Ce6 molecules tend to aggregate in aqueous media, especially under acidic conditions. In order to avoid complications of Ce6 aggregation and to simulate

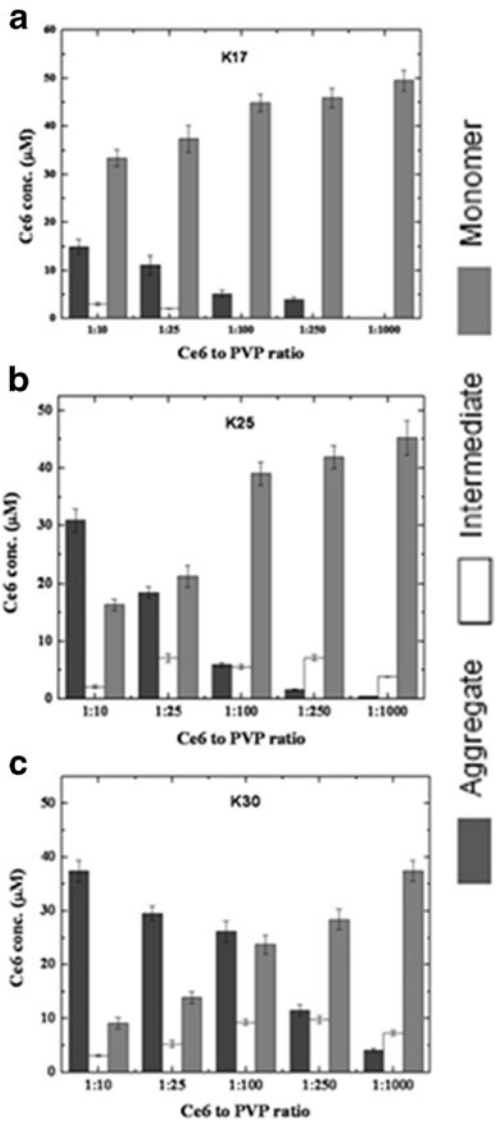

Fig. 7 Proportions of different Ce6 species present at varying Ce6:PVP ratios for PVP **a** K17, **b** K25 and **c** K30 at pH 5

physiological pH, binding of Ce6 to PVP was studied at pH 7.4. One of the efficient ways to determine the binding constant of a fluorophore involves quenching studies [34]. The fluorescence emission of Ce6 was found to decrease in the presence of PVP, suggesting a quenching-like phenomenon. However, when the decrease in fluorescence intensity was plotted against PVP concentration using the Stern-Volmer equation, it did not exhibit a linear relationship. Hence, the Stern-Volmer equation was not suitable to calculate the binding parameters. Moreover, PVP was found to be non-fluorescent in the range of 250–600 nm. Consequently, the binding parameters were determined using the Klotz plot, a model used to study the interaction between polymers and drug molecules [18]. Klotz plot describes the interaction of a ligand (drug) with a macromolecule (polymer). It is assumed that the macromolecule possesses several independent binding sites to which each ligand molecule may bind. In addition, the binding sites would be identical and should not interact with each other. The ligand and macromolecule should not undergo any chemical reaction and should exist as bound or free species. As these assumptions were met by the Ce6 and PVP employed, the Klotz plot would be a suitable Ce6-PVP binding model. According to Isakau et al., the effect of the polymer on the photophysical properties of Ce6 reached the maximum at high polymer concentration (PVP:Ce6=500:1) and henceforth became independent of the polymer content. This implied that all Ce6 molecules were bound to PVP. Therefore, the absorption spectrum of PVP bound Ce6 at PVP:Ce6 ratio of 1000:1 was taken as a reasonable experimental estimate of D_2 to calculate C_B. Fig. 8(a) shows the bound fraction of Ce6 (x) (calculated from Eqs. 3 and 4) with increasing PVP to Ce6 ratio for different PVP grades. The fraction of bound Ce6 (x) was observed to increase with increasing PVP to Ce6 ratio in a logarithmic manner ($r^2>0.96$). For a given PVP to Ce6 ratio, the fraction of PVP-bound Ce6 increased with decrease in molecular weight of PVP. All the Ce6 monomers were complexed with PVP at PVP to Ce6 ratio of 1000. Based on the fraction of PVP-bound Ce6, the number of moles of Ce6 per mole of PVP monomer unit was calculated and used in the construction of the Klotz plot. As can be seen from Fig. 8(b), all the three PVP grades generally showed good linearity in the Klotz plot. The binding parameters, K_a and n were then calculated from the slope and intercept of the Klotz plot for each of the PVP grades. The values of n was found to be smaller than 1 for the PVP macromolecule, indicating that more than one PVP monomer unit was involved in the binding with one Ce6 molecule. The p values (1/n) were calculated from the reciprocal of n. The number of probable binding sites in PVP molecule (N_0) was calculated using Eq. (6). The binding parameters, such as K_a, p and N_0 are shown in Table 1. The values of these parameters were close to those reported by Isakau et al., suggesting the applicability of a different hypothetical model (Klotz plot) to confirm the binding characteristics between Ce6 and PVP. PVP of lower molecular weight would produce a larger number of PVP molecules per unit weight of polymer. The results showed that the efficiency of binding to Ce6 was promoted by the availability of a larger number of PVP molecules, albeit shorter in chain length. PVP with a higher molecular weight will have a longer polymer chain and thus more binding sites. This aptly accounted for the high N_0 value for PVP of higher molecular weight. The increase in N_0 value was however inconsistent, probably due to polydispersity of the polymer. The number of PVP monomers per binding site, p, consistently decreased with increasing molecular weight of PVP. Increase in the p value implies association of a greater number of PVP monomers to each Ce6 molecule, resulting in strong interaction between them. The parameters determined from Klotz plot were in good agreement with those obtained by Isakau et al. using different method. In addition to binding efficiency, PVP K17 also exhibited the highest binding strength, leading to the formation of the most stable Ce6-PVP complex. According to the literature, the molecular weight of PVP for systemic use should be less than 5×10^4—8×10^4 [10]. Based on the results obtained, K17 grade will make a favourable choice for Ce6-PVP formulation.

Binding Mode Study

The thermodynamic parameters, such as enthalpy changes (ΔH) and the entropy changes (ΔS) are the main evidence to confirm binding modes. The interaction between a drug and a biomolecule may involve hydrogen bonds, van der Waals forces, electrostatic forces and hydrophobic interactions [20]. In the previous study on Ce6-PVP interaction, Isakau et al. reported the possible existence of hydrophobic interaction between Ce6 and PVP by a solubility analysis of Ce6 and its derivatives. The binding mechanism was further investigated in the present study using a more direct thermodynamic approach. From the thermodynamic standpoint, $\Delta H>0$ and $\Delta S>0$ imply a hydrophobic interaction; $\Delta H<0$ and $\Delta S<0$ reflect interaction via van der Waals forces or hydrogen bond formation; and $\Delta H\approx0$ and $\Delta S>0$ suggest an electrostatic force of attraction [35]. In this study, the effect of temperature on binding constant was studied at 15 °C, 24 °C and 37 °C. Two temperature points, one above (37 °C) and the other below (15 °C) the room temperature (24 °C), were selected to study the effect of temperature difference on the binding mechanism. Table 2 shows the binding constant values of Ce6 for different grades of PVP at the three afore-mentioned temperatures. Binding constant values were found to increase slightly for all the grades when temperature was increased from 15 °C to 37 °C. The various thermodynamic parameters, such as changes in free energy (ΔG), enthalpy (ΔH) and entropy (ΔS), were calculated using

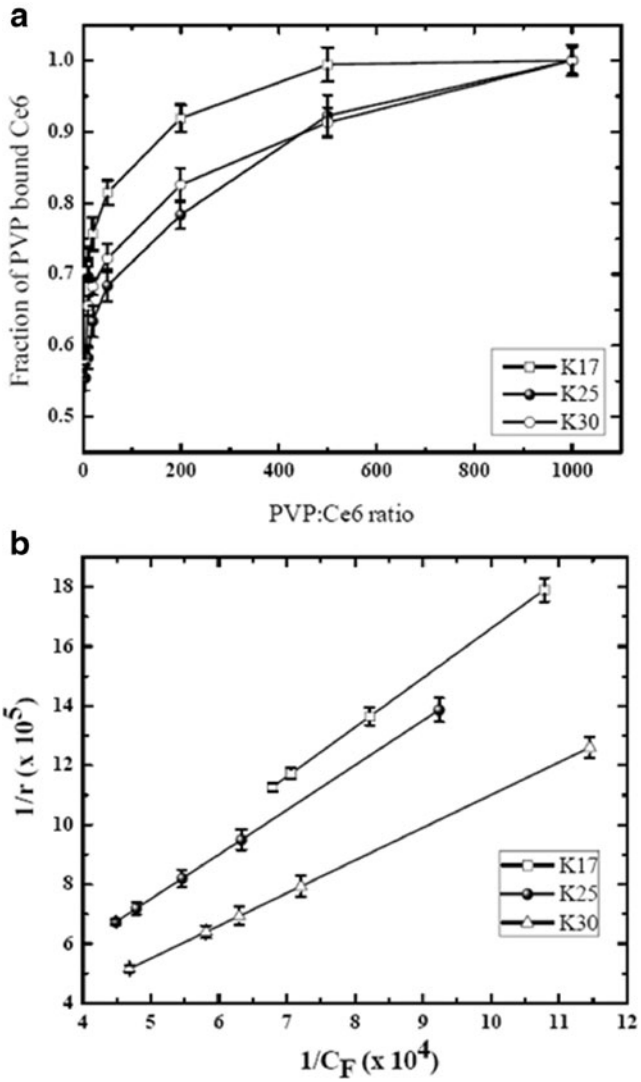

Fig. 8 **a** Effect of PVP molecular weights on the fraction of PVP-bound Ce6 and **b** fitting to Klotz reciprocal plot for different grades of PVP

Eqs. (7) and (8) and presented in Table 3. The negative values of ΔG indicate that the binding processes were spontaneous for all three grades of PVP. The positive values of ΔH and ΔS indicate partial withdrawal of non-polar groups from the medium. This observation indicates possible hydrophobic interaction between

Table 2 Variation of binding constant values with temperature for different PVP grades

PVP grades	K_a ($\times 10^4$ mol^{-1})		
	15 °C	24 °C	37 °C
K 17	3.41±0.5	3.66±0.8	3.87±0.5
K 25	3.33±0.5	3.51±0.6	3.33±0.8
K 30	3.21±0.7	3.34±0.6	3.18±0.6

Table 3 Thermodynamic parameters for binding of Ce6 with different PVP grades

PVP Grade	ΔG, 15 °C (kJ mol^{-1})	ΔG, 24 °C (kJ mol^{-1})	ΔG, 37 °C (kJ mol^{-1})	ΔH (kJ mol^{-1})	ΔS (kJ $mol^{-1}T^{-1}$)
K17	−8543	−8822	−9225	385.56	31.92
K25	−8352	−8626	−9311	290.28	30.51
K30	−8368	−8638	−9024	272.13	30.14

Ce6 and PVP, as suggested by Isakau et al. [10]. Hence, further study using molecular dynamics simulation was performed to visualize the Ce6-PVP interaction at the molecular level and elucidate the exact binding mechanism.

Molecular Dynamics Simulation

The interaction between Ce6 and PVP was further investigated by geometry optimization of Ce6-PVP system using

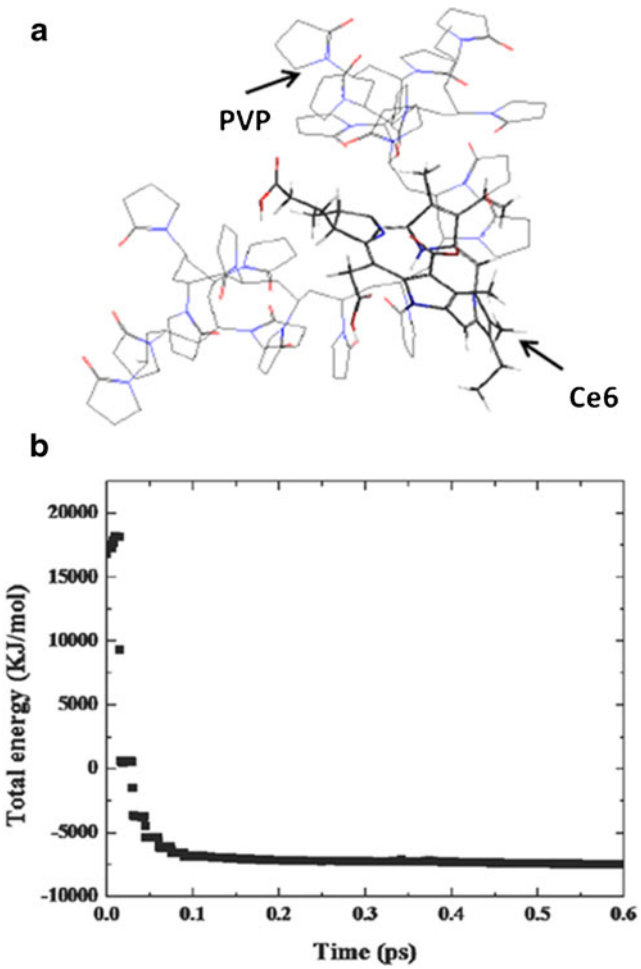

Fig. 9 Molecular dynamics simulation of Ce6-PVP system: **a** binding features of Ce6-PVP complex and **b** energy vs. time profile at the end of simulation

Hyperchem software with in-built molecular dynamics simulation [36]. The energy minimized structures of Ce6 and PVP were used for simulation within a periodic box including water molecules to simulate the experimental condition. The optimized structure of the Ce6-PVP complex at the end of the simulation is shown in Fig. 9(a). In the solvated condition, the porphyrin ring of Ce6 was found to be widened, which could be attributed to the increased mobility of the pyrrolic N-ring in the presence of the polar solvent. This facilitated the passage of PVP through the widened porphyrin macrocycle of Ce6. In the presence of the polar solvent, PVP also showed increased mobility of the pyrrolidone moieties, resulting in entanglement of the Ce6 molecule with the PVP structure. Particularly, the pyrrolidone moieties were found to be closely associated with a mean approximate distance of 6 Å from the Ce6 molecule, suggesting the possibility of hydrophobic interaction. It was possible for the PVP molecule to pass through more than one Ce6 molecule, as long as the PVP molecule involved was linear. As a consequence, the PVP molecule would present a number of PVP-binding sites for Ce6. Hence, for PVP K25 molecule with more than 100 monomer units, it could be extrapolated that more than one Ce6 molecule would be entangled with the PVP polymer. The free energy (ΔG) obtained at the end of the simulation run was found to be negative (−7,403 kJ/mol), indicating spontaneous interaction between Ce6 and PVP. The conformation of Ce6-PVP system was thermodynamically stable, as indicated by an asymptote in the energy vs. time plot (Fig. 9b), thus confirming the formation of Ce6-PVP complex through hydrophobic interaction.

Conclusion

PVP-mediated monomerization of Ce6 was found to be a function of pH and molecular weight of PVP. Ce6 aggregates existed preferentially in the pH range of 2 to 6. PVP facilitated the conversion of Ce6 aggregates into the monomeric form by forming Ce6-PVP molecular complexes. Greater monomerization of Ce6 was produced with increasing concentration of PVP. The lowest molecular weight grade (K17) exhibited highest monomerization efficiency. The complex formation mainly occurred by hydrophobic interaction between PVP and Ce6. The combination of spectroscopic, chemometric, thermodynamic and molecular simulation studies provided a valuable insight into the photophysical characteristics of Ce6 under different physiological conditions and the application of certain PVP grades to achieve optimal Ce6 activity in PDT.

Acknowledgments This research is supported by the Singapore Ministry of Health's National Medical Research Council under IRG NMRC/1187/2008 (R-148-000-114-213) and GEA-NUS PPRL fund (N-148-000-008-001). There is no conflict of interest.

References

1. Nyman ES, Hynninen PH (2004) Research advances in the use of tetrapyrrolic photosensitizers for photodynamic therapy. J Photochem Photobiol B 73:1–28
2. Brown SB, Brown EA, Walker I (2004) The present and future role of photodynamic therapy in cancer treatment. Lancet Oncol 5:497–508
3. Konan YN, Gurny R, Allémann E (2002) State of the art in the delivery of photosensitizers for photodynamic therapy. J Photochem Photobiol B 66:89–106
4. Chatterjee DK, Fong LS, Zhang Y (2008) Nanoparticles in photodynamic therapy: an emerging paradigm. Adv Drug Deliv Rev 60:1627–1637
5. Peng Q, Evensen JF, Rimington C, Moan J (1987) A comparison of different photosensitizing dyes with respect to uptake C3H-tumors and tissues of mice. Cancer Lett 36:1–10
6. Bechet D, Couleaud P, Frochot C, Viriot ML, Guillemin F, Barberi-Heyob M (2008) Nanoparticles as vehicles for delivery of photodynamic therapy agents. Trends Biotechnol 26:612–621
7. Cunderlíková B, Gangeskar L, Moan J (1999) Acid–base properties of chlorin e6: relation to cellular uptake. J Photochem Photobiol B 53:81–90
8. Kostenich GA, Zhuravkin IN, Zhavrid EA (1994) Experimental grounds for using chlorin p6 in the photodynamic therapy of malignant tumors. J Photochem Photobiol B 22:211–217
9. Zenkevich EI, Sarzhevskaya MV, Vitovtzeva TV, Kochubeev GA (1981) The regularities of aggregation and excitation electronic energy transfer in associates of pheophytin and its mesoderivatives. Mol Biol 15:145–153
10. Isakau HA, Parkhats MV, Knyukshto VN, Dzhagarov BM, Petrov EP, Petrov PT (2008) Toward understanding the high PDT efficacy of chlorine e6-polyvinylpyrrolidone formulations: photophysical and molecular aspects of photosensitizer-polymer interaction in vitro. J Photochem Photobiol B 92:165–174
11. Chin WW, Heng PW, Lim PL, Lau WK, Olivo M (2008) Improved formulation of photosensitizer chlorin e6 polyvinylpyrrolidone for fluorescence diagnostic imaging and photodynamic therapy of human cancer. Eur J Pharm Biopharm 69:1083–1093
12. Chin WW, Lau WK, Bhuvaneswari R, Heng PW, Olivo M (2007) Chlorin e6 polyvinylpyrrolidone as a fluorescent marker for fluorescence diagnosis of human bladder cancer implanted on the chick chorioallantoic membrane model. Cancer Lett 245:127–133
13. Jeong H, Huh M, Lee SJ, Koo H, Kwon IC, Jeong SY, Kim K (2011) Photosensitizer-conjugated human serum albumin nanoparticles for effective photodynamic therapy. Theranostics 1:230–239
14. Rosenkranz AA, Jans DA, Sobolev AS (2000) Targeted intracellular delivery of photosensitizers to enhance photodynamic efficiency. Immunol Cell Biol 78:452–464
15. Spikes JD, Bommer JC (1993) Photosensitizing properties of mono-l-aspartyl chlorin e6 (NPe6): a candidate sensitizer for the photodynamic therapy of tumors. J Photochem Photobiol B 17:135–143
16. Taima H, Okubo A, Yoshioka N, Inoue H (2005) Synthesis of cationic water-soluble esters of chlorin e6. Tetrahedron Lett 46:4161–4164
17. Lakowicz JR (2006) Principles of fluorescence spectroscopy, 3rd edn. Springer Publisher Co., New York
18. Maruthamuthu M, Subramanian E (1992) Polymer-ligand interaction studies. Part I. Binding of some drugs to poly(N-vinyl-2-pyrrolidone). J Chem Sci 104:417–424
19. Urios P, Rajkowski KM, Engler R, Cittanova N (1982) Investigation of human chorionic somatomammotropin-antihuman chorionic somatomammotropin antibody binding by two physicochemical

methods: phase partition and fluorescence polarization. Anal Biochem 119:253–260
20. Leckband D (2000) Measuring forces that control protein interactions. Ann Rev Biophys Biomol Struct 29:1–26
21. Parkhats MV, Galievsky VA, Stashevsky AS, Trukhacheva TV, Dzhagarov BM (2009) Dynamics and efficiency of the photosensitized singlet oxygen formation by chlorin e6: the effects of the solution pH and polyvinylpyrrolidone. Opt Spectrosc 107:974–980
22. Vermathen M, Marzorati M, Vermathen P, Bigler P (2010) pH-dependent distribution of chlorin e6 derivatives across phospholipid bilayers probed by NMR spectroscopy. Langmuir 26:11085–11094
23. Datta A, Dube A, Jain B, Tiwari A, Gupta PK (2002) The effect of pH and surfactant on the aggregation behavior of chlorin p6: a fluorescence spectroscopic study. Photochem Photobiol 75:488–494
24. SmithGJ GKP (1993) The photophysics of haematoporphyrin dimers or aggregates in aqueous solution. 1. The photophysics of haematoporphyrin dimers or aggregates in aqueous solution. J Photochem Photobiol B 19:49–54
25. De Lauder WB, Wahl P (1970) pH dependence of the fluorescence decay of tryptophan. Biochemistry 9:2750–2754
26. Weishaupt KR, Gomer CJ, Dougherty TJ (1976) Identification of singlet oxygen as the cytotoxic agent in photoinactivation of a murine tumor. Cancer Res 36:2326–2329
27. Vaupel P (2004) Tumor microenvironmental physiology and its implications for radiation oncology. Semin Radiat Oncol 14:198–206
28. Ahuja N, Katare OP, Singh B (2007) Studies on dissolution enhancement and mathematical modeling of drug release of a poorly water-soluble drug using water-soluble carriers. Eur J Pharm Biopharm 65:26–38
29. Breedveld P, Pluim D, Cipriani G, Dahlhaus F, Eijndhoven M, Wolf C, Kuil A, Beijnen JH, Scheffer GL, Jansen G, Borst P, Schellens JM (2007) The Effect of Low pH on Breast Cancer Resistance Protein (ABCG2)-Mediated transport of methotrexate, 7- Hydroxymethotrexate, methotrexate diglutamate, folic acid, mitoxantrone, topotecan, and resveratrol in in vitro drug transport models. Mol Pharmacol 71:240–249
30. Glunde K, Gugginoy SE, Solaiyappan M, Pathak AP, Ichikawaz Y, Bhujwalla ZM (2003) Extracellular acidification alters lysosomal trafficking in human breast cancer cells. Neoplasia 5:533–545
31. Levi MAB, Scarminio IS, Poppi RJ, Trevisan MG (2004) Three-way chemometric method study and UV–vis absorbance for the study of simultaneous degradation of anthocyanins in flowers of the Hibiscus rosa-sinensys species. Talanta 62:299–305
32. JiJi RD, Andersson GG, Booksh KS (2000) Application of PARAFAC for calibration with excitation-emission matrix fluorescence spectra of three classes of environmental pollutants. J Chemom 14:171–185
33. Shao LM, Zhang CY, He PJ, Lü F (2012) Comparison of different fluorescence spectrum analysis techniques to characterize humification levels of waste-derived dissolved organic matter. Environ Technol 33:2569–2573
34. Mote US, Bhattar SL, Patil SR, Kolekar GB (2010) Interaction between felodipine and bovine serum albumin: fluorescence quenching study. Luminescence 5:1–8
35. Ross DP, Sabramanian S (1981) Thermodyanmics of protein association reactions-forced contributing to stability. Biochemistry 20:3096–3102
36. Selvam S, Andrews ME, Mishra AK (2009) A photophysical study on the role of bile salt hydrophobicity in solubilizing amphotericin B aggregates. J Pharm Sci 98:4153–4160